ORIGINAL PAPER

Magnetic Resonance evaluation of tubercular lesion in spine

**Anil Kumar Jain · Ravi Sreenivasan ·
Namita Singh Saini · Sudhir Kumar · Saurabh Jain ·
Ish Kumar Dhammi**

Abstract

Purpose Information on Magnetic Resonance (MR) features of active and healed lesions in tuberculosis (TB) spine are lacking. We evaluated MRI findings in active and healed proven TB spine to establish the diagnostic features.

Materials and method Forty-nine consecutive spinal TB patients (20 male; 29 female) diagnosed clinicoradiologically and/or on histopathology, Fine Needle Aspiration Cytology (FNAC), bacteriology, or Polymerase Chain Reaction (PCR) were enrolled. Pretreatment MR scans were reviewed for diagnostic features, and eight-month follow-up MR scans were reviewed for healing changes.

A. K. Jain · R. Sreenivasan · S. Kumar · S. Jain · I. K. Dhammi
Department of Orthopedics, University College of Medical
Sciences (University of Delhi) and Guru Teg Bahadur Hospital,
New Delhi, India

R. Sreenivasan
e-mail: ravi.sreenivasan@gmail.com

S. Kumar
e-mail: profsudhirkumar@gmail.com

S. Jain
e-mail: jaindrsaurabh@gmail.com

I. K. Dhammi
e-mail: drikdhammi@gmail.com

N. S. Saini
Department of Radiology,
Institute of Nuclear Medicine and Allied Sciences,
New Delhi, India

N. S. Saini
e-mail: namita23m@gmail.com

A. K. Jain (✉)
A-10 Part B, Ashok Nagar,
Ghaziabad, Uttar Pradesh, India
e-mail: dranilkjain@gmail.com

Results Cervical spine (*n*=6), dorsal spine (*n*=14), and lumbar spine (*n*=29) were affected. Fourteen had paraplegia. Mean vertebrae involved were 2.61 on X-ray with a total of 128 vertebrae (VB) and 3.2 on MRI (range, 2–15) with 161 VB. The lesions were more extensive on MRI (34.7%) than appreciated on X-ray. The disc was preserved partially or fully in 88.2% of instances. End plate erosions (159/161 VB), lost VB height (94/161), exudative lesion (158/161), granular lesion (3/161), pre and paravertebral collections (49/49 cases), marrow oedema (161/161), discitis (98%), epidural involvement (107/161), epidural spread (100/161), and subligamentous spread (156/161) were observed. Canal encroachment (10–90%) was seen in 37 cases. Mean motor and sensory scores with greater than 50% canal encroachment were 87/100 and 156/168, respectively. Cord oedema was observed in 11 cases (eight with neural deficit and three cases without). Cord atrophy was seen in one case each before and after treatment. A total of 83% of patients had a combination of paravertebral collections, marrow oedema, subligamentous and epidural extension, endplate erosions and discitis. On healing (*n*=20), complete resolution of marrow oedema and collections, fatty replacement of bone marrow and resolution of cord signal intensity were observed.

Conclusion The marrow oedema, preservation of disc space, subligamentous extension of abscess, septate paravertebral abscess, epidural extension, endplate erosions and discitis were consistently observed in 83% cases of TB spine on MRI.

Introduction

Early diagnosis of spinal tuberculosis (TB) can prevent development of spinal deformity and neurological complications. A histopathological/bacteriological/cytological diagnosis

is not always possible in a deep seated lesion; hence imaging is an important modality for the diagnosis of spinal tuberculosis.

It takes nearly three to four months for a spinal TB lesion to show up in plain radiographs [1, 2]. MRI is sensitive for early detection of inflammation and consequent diagnosis of spinal TB in view of its excellent contrast resolution and multiplanar capabilities with equally good definition of bone and soft tissues [2–4].

MRI features are described in active and healed disease as well as cord changes in tuberculous paraplegia [1, 3–8]. However, there is a lack of consensus on what constitutes the characteristic features of a tubercular lesion in the spine. Hence this study aims to evaluate MRI findings in proven cases of spinal TB in active and healed stages of disease.

Materials and methods

Forty-nine patients with paradiscal spinal TB lesion, with/without paraplegia, aged over ten years were enrolled. All patients having classical clinicoradiological diagnosis of spinal tuberculosis who showed evidence of healing on treatment, or with a proven histopathological/bacteriological/cytological diagnosis of TB spine were included in the study. The cases were (a) freshly diagnosed cases of TB spine (group A) (b) patients who had completed treatment successfully and had a pre treatment MR scan (group B).

Patients with atypical presentations of TB spine such as isolated intraspinal granuloma, isolated posterior complex involvement, single vertebral body lesion, isolated craniovertebral junction TB, isolated sacral tuberculosis or patients without a classical clinicoradiological diagnosis were excluded from the study. Neurological assessment was performed by Jain and Sinha scoring system [9]. Full blood count, ESR, LFT and KFT were performed on admission.

The radiological diagnosis was made on observations of demineralisation of the vertebra, fuzzy paradiscal margin, reduction/obliteration of disc space, along with one or more of the following: destruction of end plates, wedging of vertebra, obvious kyphotic deformity, paravertebral shadows, and anterior scalloping of verterbral body. The aspirate of paraspinal and psoas abscesses (n-9) was sent for Z-N staining, pus culture, and PCR. CT guided biopsy was done in two patients. The surgical decompression (with or without instrumented stabilisation) was done for severe neurological deficits, developing or progressive neural deficits on treatment, panvertebral disease and severe kyphotic deformity. The tissue was sent for histopathological examination. Pus and granulation tissue were sent for Z-N staining, tubercular culture and PCR.

In all prospective patients, MRI was performed pretreatment and repeated after eight months. The MR imaging was performed on different systems with magnetic field strengths ranging from 1 to 3 Tesla. Sagittal, axial and coronal T1-weighted spin-echo images and T2-weighted fast spin-echo images were obtained using phased array/matrix coils. Additional coronal and sagittal STIR fat suppression sequence images were also obtained.

MR findings in an active lesion

The bone marrow oedema was defined as hypointense signal intensity on T1WI and hyperintense on T2WI, and caseous exudative type as mildly hyperintense in T1WI and T2WI and granular type as heterogeneous hypo or hyperintensity in T2WI. Evidence of ischemic necrosis with vertebral body destruction was seen as altered signal intensity in the body in both T1 and T2 images.

The end plate erosion was defined as irregularity of margins of verterbral body endplates. Loss of vertebral body height was defined as decrease in the average vertebral body height on comparison with adjacent uninvolved normal vertebrae.

Reduction in disc height was defined as decrease in the average disc height in comparison with adjacent uninvolved normal discs. The discitis was defined as hyperintense signal in T2WI in the disc with loss of intranuclear cleft and/or reduction in disc height and enhancement of the disc margins on post contrast T1WI.

Presence of paravertebral collections as low signal on T1WI and hyperintense signal on T2WI along with extent and location of collection was noted. Calcification if present was seen as signal void in all sequences. Subligamentous spread was defined as spread of pus beneath the anterior longitudinal ligament. The vertical extent and location of subligamentous and epidural collections were noted. Intradural abscess was defined as pus seen as hyperintense in T2WI and hypointense in T1WI within the dural sheath. Presence of psoas abscess was also noted. Epidural component was defined as epidural indentation/canal encroachment by pus/granulation tissue. Epidural spread was defined as spread of pus within the vertebral canal outside the dura beyond a single vertebral level. Presence of epidural spread implies presence of epidural component but not vice versa.

Percentage canal encroachment was calculated on axial images by dividing the spinal canal into four quadrants by drawing a vertical line and then drawing a perpendicular bisector line to the same and assessing the occupancy of the cord and the encroachment in each quadrant subjectively. Greater than 10% encroachment was taken as significant. Nerve root compression was defined as any impingement on the nerve with the loss of perineural fat planes. Nerve root clumping was defined as peripherally splayed out or centrally clumped nerve roots seen in cases of arachnoiditis.

Intramedullary granuloma was defined as ring enhancing lesion within the spinal cord on contrast MRI. Intradural granuloma was defined as ring enhancing lesion within the dural sheath separate from the substance of cord.

Spinal cord changes: Cord oedema was seen as hyperintense signal on T2WI and hypointense on T1WI within substance of cord. Cord atrophy was seen as decreased cord girth on axial sections with decreased canal occupancy and increased space surrounding the cord. Myelomalacia seen as focal area of altered signal intensity that appears hypo-intense on T1WI and hyperintense on T2WI without cord expansion. Syringomyelia was seen as enlarged/dilated central spinal canal. Arachnoiditis was seen as enhancement of dura arachnoid in post contrast images with clumping of nerve roots. Thickening of dura-arachnoid complex was seen as enhancement of dura-arachnoid in post contrast images.

MR findings on healing

The healing of the vertebral lesion was recorded on complete resolution of marrow oedema, replacement of marrow by fat seen as a bright signal on T1WI and T2WI and complete resolution of paravertebral collections.

All group A cases were put on Anti Tuberculous Therapy (ATT) regimen as per Directly Observed Treatment Short course (DOTS) Category I which consisted of alternate day dosage (thrice weekly) with rifampicin [R] (10 mg/kg), isoniazid [H] (10 mg/kg), pyrazinamide [Z] (35 mg/kg), and ethambutol [E] (30 mg/kg) [10]. The dosage schedule was HRZE for two months followed by HR for the next six months [10]. Patients who had already had ATT in the recent past for pulmonary or extra-pulmonary disease were put on Category II treatment which consisted of HRZES for two months followed by HRZE for one month and HR for another six months. Injection of streptomycin [S] was given at a dosage of 750 mg IM (15 mg/kg, maximum 1 g). Cases already on treatment on non-DOTS were continued on the same.

Patients were followed on a monthly basis. Neural improvement in the outcome was documented. At the completion of DOTS regimen they were subjected to a repeat MR scan for evaluation. The patients who had achieved healing were monitored for any signs of recurrence or relapse every six months.

Results

Thirty-two patients were enrolled in group A and 17 patients in group B. There were 20 males and 29 females with mean age 30.69 years (11–70 years). The cervical spine (n-6), dorsal spine (n-14) and lumbar spine were affected in 29 cases. Seven patients had multilevel contiguous involvement spanning two

or more regions on MRI. Kyphotic deformity was seen in 18 patients with mean K angle of 30 degrees. Five patients underwent deformity correction and instrumented stabilisation. Three patients underwent surgical decompression only. The mean pretreatment ESR was 56.59 mm FHR (range, 11–110) which decreased to 25.81 mm FHR (range, 3–56) after eight months of treatment ($p<0.001$) in 37 patients on follow-up. Twenty-six patients were diagnosed on clinicor-adiological grounds and healing response to antitubercular treatment. The diagnosis of tuberculosis was confirmed in 23 cases with either histopathology, FNAC, smear, culture, or PCR. Nine patients had more than one diagnostic test positive.

On radiographs, 49 patients had 51 lesions (two skip lesions); 39 had two VB lesion while 9, 2 and one had three, four, and 15 VB involvement, respectively. On MRI it showed 49 contiguous lesions; 25 had two VB lesions while 12 (three VB), six (four VB), one (six VB), two (seven VB), two (eight VB) and one had 15 VB involvement. The average vertebrae involved on X-rays were 2.61 (range 2–15, total 128 VB) while on MRI the average VB involvement was 3.29 (range 2–15, total 161 VB). In 17/49 (34.7%) cases MRI revealed a greater number of VB involved than on X-ray (Figs. 1, 2). The marrow oedema was observed in all 49/49 cases (161/161 VB) with 11/49 lesions showing heterogeneous signal suggestive of areas of caseation and abscess. Since contrast was not administered, the diagnosis of intra-osseous abscess could not be made. The anterior and central column involvement was seen in all patients.

Demineralisation was observed in 124/128 VB. Endplate erosions and fuzzy paradiscal margins were seen in 125/128 VB levels on X-rays. There were 154 endplates; 26 endplates (13 discs obliterated) were completely destroyed, 122 (95.3%) endplates showed erosions, and six (4.7%) endplates were spared. On MRI the endplate erosions were seen in 159/161 VB levels. The total endplates were 220; 192/194 (99%) endplates showed erosions; 26 endplates (13 discs) were destroyed and two (1%) endplates were spared. Wedging and varying degree of VB height loss was seen in 63/128 (50.8%) VB in 34 patients on X-ray while MRI revealed the same in 94/161 (58.4%) VB in 45 patients. A total of 64/77 (83%) disc spaces were narrowed and 13/77 (17%) discs were obliterated on X-rays while on MRI 13 discs were not discernible and 97 (88.2%) discs were intact with preserved disk signal with slight reduction of disk height in 95/97 discs. Discitis was seen in 95/97 (98%) preserved discs. As contrast was not administered, disc abscess with rim enhancement was not typically seen in any case.

Paraspinal shadows were seen in 39/49 (79.6%, 107 diseased VB) patients on X-ray with a vertical extent of 128 VB. On MRI an exudative type (48/49 patients with 158/161 VB) and granular type (n-1,3/161 VB) were observed. The
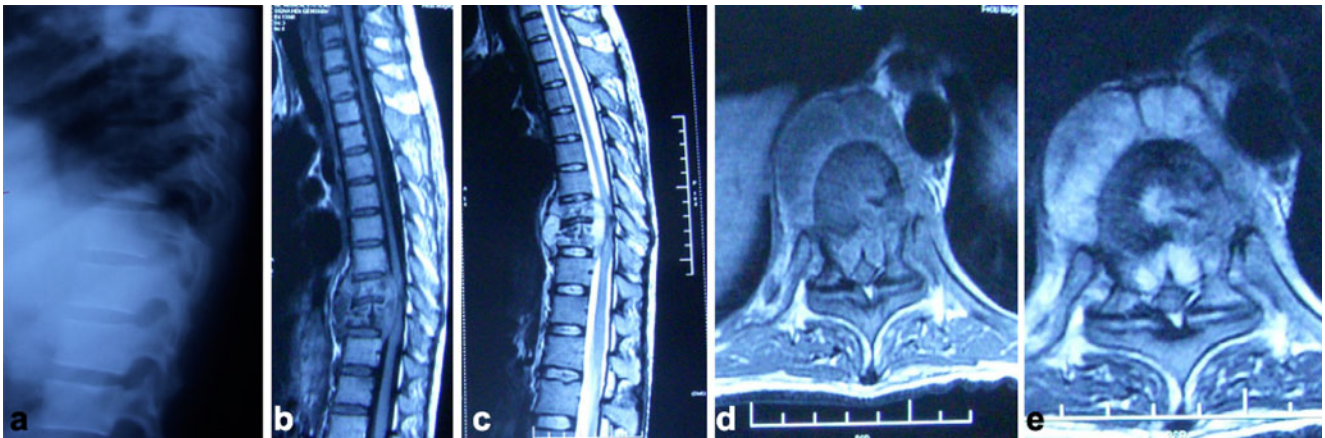
Fig. 1 **a** Plain X-ray lateral view shows paradiscal lesion D9D10 with destroyed paradiscal margins with endplate erosions and decrease in vertebral height of D10. **b, c** Sagittal section T1W and T2W show paradiscal lesions with intraosseous caseation with preserved discs with anterior subligamentous spread of prevertebral collection with anterior epidural spread of collection compressing spinal cord. **d, e** Axial section T1W and T2W show large septate prevertebral collection, intraosseous caseation with large anterior epidural collection and 75% canal encroachment

septate and loculated pre and paravertebral collections were observed in 49 (100%) cases with vertical extent of 186 VB (mean 3.80, SD 2.47, range two to 15) more than the number of vertebral bodies involved. Nine of 49 (18.36%) patients had psoas abscesses. Subligamentous spread of abscess beneath the anterior longitudinal ligament was seen in 45/49 (92%) cases in 156/161 (96%) VB levels. Epidural involvement was seen in 42/49 (86%) cases with vertical extent of 107/161 (66.2%) VB levels with epidural spread of exudate in 34/49 cases with vertical extent of 100/161 VB levels. No case of intradural abscess or intradural extramedullary granuloma was found. An intramedullary granuloma in one patient with mild neural deficit resolved following treatment on follow-up MR scan at eight months. Nerve root compression/encasement by disease was seen in 30/49 (61.22%) of cases.

Thirty-five patients had no neurological deficits while 14 had paraplegia of varying severity. The canal encroachment was observed in 37/49 (75.5%) cases with mean 28.98 (SD 25.03, range 10–90%). The mean percentage canal encroachment was 42.14% (range, 10–80) in 14 cases of paraplegia, and 35% (range, 10–90%) in 23 cases without paraplegia. Fourteen patients had over 50% canal encroachment. Eight (six dorsal, one cervicodorsal, one lumbar) out of the 14 patients had paraplegia with mean motor score of 77 (range, 50–96) and mean sensory score of 147.25 (range, 132–168). The remaining six (four lumbar, one cervical, one dorsal) had no neural deficit.

We found oedema of the spinal cord in 11/49 (22.4%) cases out of which eight (one cervical, six dorsal, one lumbar) had neural deficit with mean pre treatment motor and sensory scores of 66.5/100 (range, 50–82) and 140/168 (range, 94–168), respectively. On follow-up MRI six showed complete resolution of cord oedema and neural deficit.

Cord atrophy was observed in two cases. One case with pre treatment motor and sensory scores of 50 and 94, respectively, attained motor and sensory scores of 80 and 168 on treatment. The other case developed cord atrophy on completion of treatment. We did not find myelomalacia, syringomelia arachnoiditis, thickened arachnoid complex and meningeal involvement as contrast was not administered to any patient for their pre-treatment MRI.

Twenty-eight patients in group A and 11 in group B were treated by DOTS regimen while four in group A and six in group B by daily dosage ATT regimen. Twenty patients on follow-up were declared healed with ten in both groups. Seventeen were declared healed on observation of complete loss of marrow oedema, resolution of paravertebral collections and replacement of vertebral body marrow by fat (Figs. 2 and 3). Two patients had ambiguous MR picture and were declared healed on observing no [18]F- FDG uptake on PET Scan. One patient continued to have persistent activity in her psoas despite healed vertebral disease.

Discussion

The sensitivity, specificity and accuracy of plain X-rays are 82%, 57% and 73%, respectively, for diagnosis of spinal TB [11]. The X-rays are unable to visualise accurately the "blind areas" (cranio-vertebral junction, cervico-dorsal region, sacrum, sacro-iliac joints, posterior elements) due to overlapping of shoulder shadows [11, 12]. CT does delineate bone destruction earlier than X-rays. The tissues for AFB smear, histology and PCR can establish the diagnosis with certainty. It may need major surgical procedures to procure tissue in deep seated spinal lesion [2, 12]. PCR is not indicative of disease activity as positive results have been obtained from samples of fossilized bone tissue as well [13].
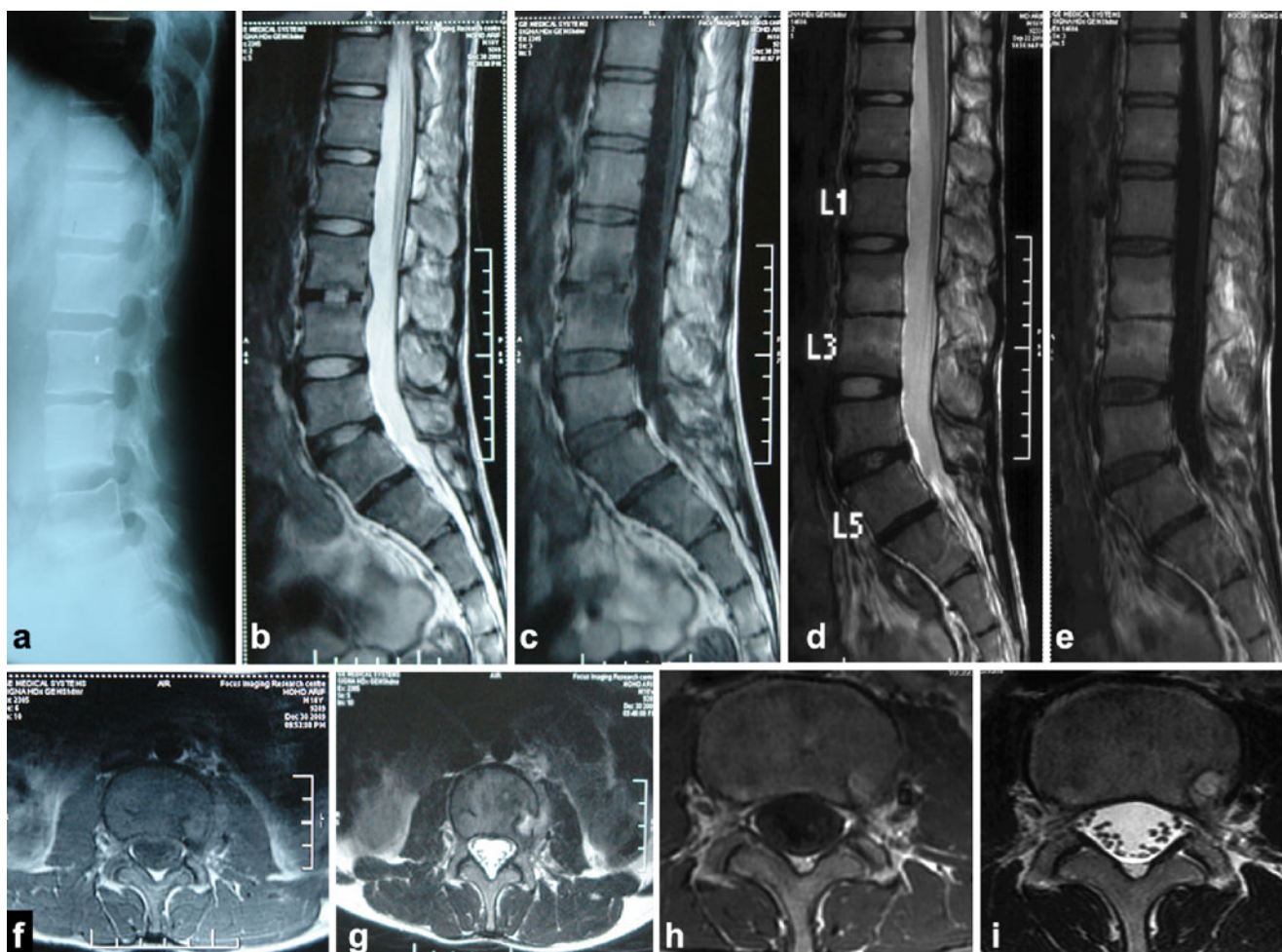
Fig. 2 **a** Plain X-ray lateral view (pretreatment) shows decreased disc space in L2-L3 vertebral bodies. **b** Sagittal section of T2W MRI shows paradiscal lesion (hyperintense signal suggestive of marrow oedema) in L2-L3 with discitis with small anterior epidural collection. **c** Sagittal section of T1W MRI shows hypointense signal in L2-L3 paradiscal region. **d**, **e** Eight months nonoperative post-treatment MRI scan sagittal section T2W and T1WI shows resolution of anterior epidural collection and bone oedema. Hyperintense signal in L2-L3 VB suggestive of fatty infiltration of marrow. **f**, **g** Pretreatment axial T1WI and T2WI show a thin rim of paravertebral collection towards the left side with evidence of bone oedema, which has resolved on post treatment axial T1WI (**h**) and T2WI (**i**)

MRI is more sensitive than radiography and more specific than scintigraphy in the diagnosis of spinal TB, as it detects soft tissue lesions earlier and can demonstrate soft tissue and vertebral body involvement, subligamentous spread of pus, spinal canal and cord changes and compression (extradural and intradural) along with specific changes related to healing due to its excellent soft tissue contrast resolution. It has multiplanar capabilities with no hazard of radiation. With the advent of non-ferromagnetic titanium implants, MRI can be safely used in patients who have undergone instrumentation and have implants in-situ [7].

The radiological delay in diagnosis of spinal TB can be avoided if we can diagnose tubercular spondylitis, based on certain characteristic features, on MRI before it can be seen on a plain radiograph. Various authors have reported a select number of MRI findings in a limited number of patients which lacks uniformity of terms and descriptions [1, 2, 5–8, 14–24]. This study was undertaken to document all MR features in proven cases of spinal tuberculosis

Chronic localised back pain of varying severity and duration was the presentation. The elevated ESR reduced significantly after eight months of ATT. Hoffman et al. [16] reported pre-treatment ESR of 76 mm FHR (n-25); 26 (54%) of our patients were diagnosed clinicoradiologically and response to ATT, and 23 cases (46%) were diagnosed with either histopathology (14/14), FNAC (5/5), smear+ culture (10/15-smear and 5/15-culture) or PCR (9/10) giving a diagnostic yield of 66% and 33% for smear and culture, respectively, which lies within the reported values of 25–75% for smear and is lower than 40–88% for culture [12] (Table 1).
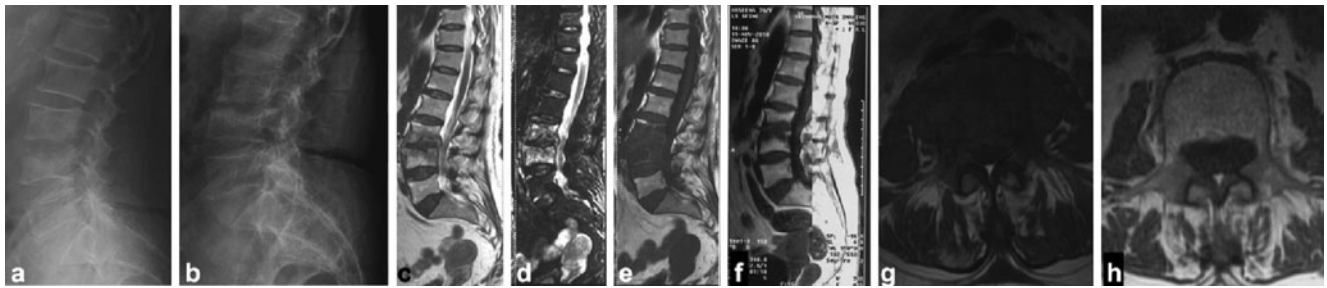
Fig. 3 a Plain X-ray lateral view (pre treatment) shows erosion of endplates with fuzzy paradiscal margins (L4) with loss of vertebral height in L3, L4. **b** Plain X-ray lateral view (8 months post-treatment) shows sclerosis of endplate of L3, L4 with sharpening of paradiscal margins. **c,d,e** Pre treatment sagittal section T2W, STIR and T1W shows paradiscal lesion L3,L4 with anterior subligamentous spread with a small anterior epidural collection with discitis and preserved discs. Marrow oedema is seen as a hyperintense signal on STIR. **f** Eight months post treatment sagittal T1WI shows resolution of collections with hyperintense signal in T1WI suggestive of fatty marrow infiltration. **g** Pretreatment axial T1W image shows presence of hypointense signal and paravertebral collections. **h** T1WI axial scan of the same patient at 8 months posttreatment shows resolution of paravertebral collections with hyperintense signal in VB suggestive of fatty replacement of marrow as evidence of healing

Neurological deficit was seen only in 14 cases (28.75%). Desai [1], Hoffman et al. [16] and Kim et al. [18] had also reported back pain as a consistent finding in more than 90% of patients and only 30–40% with neural involvement. Andronikou et al. [5] reported neural deficit in 75% of his patients. The mean percentage canal encroachment seen on MRI, in 14 patients with paraplegia, was 58.75% on MRI (range 50–80) whereas in 23 cases without paraplegia it was 35% (10–90%). Hoffman et al. [16] correlated 60% canal encroachment in a mid sagittal MR scan with neural deficits. Jain had reported that up to 76% canal encroachment is compatible with an intact neural state if any other cause such as spinal instability does not exist [2, 25].

The lesion was more extensive on MRI than was seen on X-rays as also reported by Smith et al. [15] and Hoffman et al. [16] in 4/4 and 6/25 cases, respectively. Reported incidence of contiguous VB involvement include Smith et al. [15] (2/4, 50%), Liu et al. [17] (27/29, 93.1 %), Desai [1] (11/24, 45.8%; 12 patients had a single VB lesion), Jung et al. [24] (12/20, 60%), Andronikou et al. [5] (45/53, 84.9%), Sinan et al. [14] (10/11, 90.9 %), and Loke et al. [21] (12/15, 80%), since most authors have not excluded single vertebral lesion; hence, they have reported a variable percentage of contiguous lesions while we have excluded single VB lesions.

Marrow oedema was observed in 161/161 affected VB. Other series have also reported almost 100% incidence of marrow oedema in cases of TB spine [1–9, 16–33]. The caseous exudative type was more common (48/49 cases, 158/161 VB) while 3/161 (1.86%) VB had the granular type (Table 2). On X-rays disc space was uniformly decreased in all patients while on MRI 97 of 110 had fully preserved disc albeit with reduced height. Discitis was observed in 95/97 (98%) preserved discs. Joseffer et al. [26], Mahboubi et al. [27] and Jain et al. [34] stated that preservation of discs despite extensive bone destruction is virtually pathognomonic for spinal TB. It has been postulated that mycobacteria lack the proteolytic enzymes found in bacteria that cause pyogenic osteomyelitis and this may be responsible for the relative sparing of the disc. The avascularity of the discs may prevent them from serving as an initial site of infection and disc destruction begins only when the two adjacent VBs are so structurally weakened that the disc not only loses its nutritional support but it also herniates into the soft vertebral body, seen as loss of interverbral disc on X-rays [34, 35]. Various authors have reported varying incidence of disc preservation including Yusof et al. [22] (63% destroyed, 34% spared), Chang et al. [8] (42.4% destroyed, 57.6% spared), Liu et al. [17] (72.4% destroyed, 27.5% spared), Desai [1] (50% disc space reduced, 50% spared), al-Mulhim et al. [20] (46% destroyed, 54% spared), Loke et al. [21] (63.6% destroyed, 36.4% spared), Akman et al. [6] (77.3% discitis, 22.7% spared), Andronikou et al. [5] (100% involved with 100% disc height reduction), Jung et al. [24] (55% disc space narrow, 45% disc space preserved, 80% had discitis), and Thrush et al. [23] (100% spared).

Forty-eight (98%) cases of X-rays as well as MRI showed endplate erosions and fuzzy paradiscal margins. Reported incidences of endplate erosions by various workers include Smith et al. [15] (1/4, 25%), Thrush et al. [23] (3/3, 100%), Liu et al. [17] (22/29, 75.8 %) and Chang et al. [8] (33/33, 100%).

Wedging and varying degree of VB height loss was seen in 63/128 (49.2%, 34/49 patients) VB on X-ray. MRI revealed the same in 94/161(58.3%, 45/49 patients) VB. Demineralisation was seen in 124/128 (96.8%) VB on X-ray. Scoliotic deformity was seen in five patients whereas 18 showed kyphotic deformity with mean kyphotic angle of 30 degree (range 5–56°). Yusof et al. [22] reported kyphosis in 26 (84%) patients with TB spine with a mean

Table 1 Distribution of investigation findings in 23 cases where tissue was procured

Serial number	Name	Diagnostic tests				
		Histopathology	FNAC	Smear	Culture	PCR
1	A2			+	-	+
2	A4	+	+	-	-	+
3	A6			-	-	+
4	A8		+	-	-	
5	A12			+	-	
6	A13			-	-	+
7	A14			+	-	
8	A16			+	-	
9	A21	+				
10	A23	+	+	+	+	+
11	A25			+	-	
12	A27	+				+
13	A29	+				
14	A31	+		+	+	+
15	A32	+		-	+	
16	B3	+				
17	B4	+	+	+	+	+
18	B5	+				
19	B6	+				
20	B7	+	+	+	-	
21	B8			+	+	+
22	B9	+				
23	B11	+				

angle of kyphosis of 15°. Chang et al. [8] reported 20/33 patients with mean K angle of 17.9° on X-rays and 14.8° on MRI.

The pre and paravertebral abscesses are reported between 58 and 100% with most workers reporting almost 100% involvement. The pre and paravertebral septate loculated collections with the extent more than the number of vertebral bodies involved was observed in our study in 49 (100%) cases. Loke et al. [21] stated that the presence of an air fluid level in paravertebral collections virtually excluded TB, due to the chronicity of the disease. We did not find any in our cases.

Subligamentous spread of abscess beneath the anterior longitudinal ligament was seen in 45/49 (92%) cases and 156/161 (96.8%) VB levels (Table 2). This has been reported to be characteristic of TB spine by Liu et al. [17] (27/29, 93%), Desai [1] (15/24, 62.5%), Andronikou et al. [5] (34/53, 64%), Jung et al. [24] (17/20, 85%), Chang et al. [8] (24/33, 73%), Yusof et al. [22] (17/31, 58%), and Loke et al. [21] (10/15, 66%). Nine of 49 (18.36%) patients had additional psoas abscesses. de Roos et al. [29] observed psoas abscesses in 4/4 (100%) patients. Lindahl et al. [30] also reported the presence of psoas abscess as characteristic of TB spine.

The epidural involvement is reported between 53.3% (Loke et al. [21]; n=15) and 100% (Thrush et al. [23]; n=3) and the epidural spread between 45% (Chang et al. [8]; n=33) and 93% (Andronikou et al. [5]; n=53). Epidural involvement was seen in 42/49 (85.71%) cases with a vertical extent of 107/161 VB levels with epidural spread of exudate in 34/49 (69, 39%) cases with vertical extent of 100/161 VB levels (Table 2).

We did not find any case of intradural abscess or intradural extramedullary granuloma; however, an intramedullary granuloma was seen in one patient which resolved following treatment on follow-up MR scan at eight months (Table 2). Desai [1] had reported an extradural granuloma in 6/24 (25%) cases. Dhammi et al. [31] and Jena et al. [32] reported intramedullary granuloma in tubercular spine which resolved on ATT.

Canal encroachment was observed in 37/49 (75.5% paraplegic [n-14] and 23 non paraplegic) cases varying between ten and 90% (mean 28.9) (Table 2). Jain reported up to 76% canal encroachment to be compatible with an intact neural state [25]. Hoffman et al. [16] found that canal encroachment of 60% or more above the level of conus resulted in paraplegia. Liu et al. [17] found 93% of cases to have canal encroachment (cord indentation);

Table 2 Summary of MRI findings

Patient number	Parameter	VB extent, $N=161$	Number of cases, $N=49$
1	Exudative picture	158	48
2	Granular picture	3	1
3	Psoas abscess		9
4	Septate loculated collections		49
5	Subligamentous spread	156	45
6	Epidural component	107	42
7	Epidural spread	100	34
8	Intramedullary granuloma	1	1
9	Nerve root compression/encasement		30
10	Canal encroachment		37
11	Internal bony salient due to proximal VB		9
12	Internal bony salient due to distal VB		2
13	Cord compression		14
14	Cord oedema		11
15	Cord atrophy		2
16	Myelomalacia/Syrinx		0

however, the neurological status of their patients was not described.

We found altered cord signal intensity in 11/49 (22.4%) cases (Table 2). The oedema of the cord is compatible with good neurological recovery following treatment, while myelomalacia, accompanied by a severe neurological deficit, may show incomplete recovery [9]. Mild atrophy of the cord is observed even after successful neurological outcome, whereas moderate to severe atrophy, with or without syringohydromyelia, is seen in late-onset paraplegia [12, 22]. We did not find myelomalacia or syringomelia in any case since none of our patients had long-standing paraplegia. when such cord changes are manifest. We could not appreciate arachnoiditis, thickened arachnoid complex and meningeal involvement as contrast was not administered to any patient for their pre-treatment MRI.

Seventeen out of 20 patients were declared healed on follow-up MRI on complete loss of marrow oedema, resolution of paravertebral collections and replacement of vertebral body marrow by fat as seen as increased signal on T1-weighted images. Similarly, features were suggested by Smith et al. [15], Sharif et al. [3], and Hoffman et al. [16]. Gillams et al. [33] concluded that a high signal intensity rim on T1 weighed images at the edge of lesion was suggestive of healing, and reconstituted marrow was fatty and appeared to have equal intensity at both T1 and T2 phases. They also added that progressive reduction and complete disappearance of gadolinium enhancement of bone lesions and of soft tissue is highly suggestive of healing lesion.

None of the patients had a contrast scan done which limited the study of certain parameters that are appreciated only on administration of contrast. We did not use contrast as the diagnosis was never in doubt and there were logistical issues about the availability and affordability of contrast material. The delineation of abscess wall, meningeal inflammation (arachnoiditis), disc abscess and intra-osseous abscess are better appreciated on Gd-DTPA contrast enhanced MR scan [24].

All (100%) cases had a combination of marrow oedema and paravertebral collections. A total of 92% had marrow oedema and subligamentous spread of disease; 98% of cases had marrow oedema, paravertebral collections and endplate erosions. Endplate erosions, subligamentous spread, marrow oedema and paravertebral collections were seen in 91.8%. A total of 83% had subligamentous spread and epidural components suggestive of spread anterior and posterior to the VB; 83% had paravertebral collections, marrow oedema, subligamentous and epidural extension, endplate erosions and discitis.

Jung et al. [24] found a combination of a well-defined paraspinal abnormal signal and thin, smooth abscess wall in 90% of instances in TB spine as compared to 0% in pyogenic. Danchaivijitr et al. [7] believe that high sensitivity and specificity are a disruption of the endplate, at 100% and 81.4%, respectively, as well as a paravertebral soft-tissue shadow (96.8%, 85.3%) and a high signal intensity of the intervertebral disc on the T2WI (80.6%, 82.4%). Shanley [19] states that vertebral intraosseous abscesses, skip lesions, subligamentous spread of infection, and epidural extension are commonly associated with tuberculous spondylitis and the presence of a thick rim of enhancement around paraspinal and intraosseous abscesses are reported to be diagnostic. Chang et

al. [8] state that the most distinctive MRI findings of tuberculous spondylitis are mainly a pattern of bone destruction with relative disc preservation, focal and heterogeneous enhancement, well-defined abnormal signal intensity in paraspinal areas and an intraosseous abscess with rim enhancement. Liu et al. [17] concluded that a combination of contiguous involvement of ten VB, subligamentous spread, endplate erosions, low T1W and high T2W was suggestive of TB.

In conclusion, one can diagnose the tubercular spondylitis earlier with confidence, on presence of specific characteristics, on MRI. Involvement is seen to be more extensive in MRI than on X-rays. Marrow oedema (100%), pre and paravertebral septate loculated collections (100%), subligamentous collections (92%) and endplate erosions (99%) with epidural extension are among the most consistent findings in tubercular spondylodiscitis seen on MRI. Preservation of discs despite extensive bone destruction is virtually pathognomonic for spinal TB. The canal encroachment could not be correlated with neural deficit. The cord oedema is found compatible with good neural outcome. The resolution of bone oedema, paravertebral abscess and fatty replacement of bone marrow are observed with healing of TB lesion of the spine.

Conflict of interest The authors have no conflicts of interest to report.

References

1. Desai SS (1994) Early diagnosis of spinal tuberculosis by MRI. J Bone Joint Surg Br 76(6):863–869
2. Jain AK (2010) Tuberculosis of the spine: a fresh look at an old disease. J Bone Joint Surg Br 92-B:905–913
3. Sharif HS, Clark DC, Aabed MY, Haddad MC, al Deeb SM, Yaqub B, al Moutaery KR (1990) Granulomatous spinal infections: MR imaging. Radiology 177(1):101–107
4. Jain AK (2002) Treatment of tuberculosis of the spine with neurologic complications. Clin Orthop Relat Res (398):75–84
5. Andronikou S, Jadwat S, Douis H (2002) Patterns of disease on MRI in 53 children with tuberculous spondylitis and the role of gadolinium. Pediatr Radiol 32(11):798–805
6. Akman S, Sirvanci M, Talu U, Gogus A, Hamzaoglu A (2003) Magnetic resonance imaging of tuberculous spondylitis. Orthopedics 26(1):69–73
7. Danchaivijitr N, Temram S, Thepmongkhol K, Chiewvit P (2007) Diagnostic accuracy of MR imaging in tuberculous spondylitis. J Med Assoc Thai 90(8):1581–1589
8. Chang MC, Wu HT, Lee CH, Liu CL, Chen TH (2006) Tuberculous spondylitis and pyogenic spondylitis: comparative magnetic resonance imaging features. Spine (Phila Pa 1976) 31(7):782–788
9. Jain AK, Jena A, Dhammi IK (2000) Correlation of clinical course with magnetic resonance imaging in tuberculous myelopathy. Neurol India 48(2):132–139
10. WHO (2010) Global tuberculosis control: WHO report 2010. WHO, Geneva
11. Tuli SM (2004) Tuberculosis of the skeletal system, 3rd edn. Jaypee Brothers Medical Publishers, New Delhi, India
12. Negi SS, Khan SF, Gupta S et al (2005) Comparison of the conventional diagnostic modalities, BACTEC culture and poly-merase chain reaction test for diagnosis of tuberculosis. Indian J Med Microbiol 23:29–33
13. Zink AR, Grabner W, Nerlich AG (2005) Molecular identification of human tuberculosis in recent and historic bone tissue samples: the role of molecular techniques for the study of historic tuberculosis. Am J Phys Anthropol 126:32–47
14. Sinan T, Al-Khawari H, Ismail M, Ben-Nakhi A, Sheikh M (2004) Spinal tuberculosis: CT and MRI feature. Ann Saudi Med 24:437–441
15. Smith AS, Weinstein MA, Mizushima A, Coughlin B, Hayden SP, Lakin MM, Lanzieri CF (1989) MR imaging characteristics of tuberculous spondylitis vs. vertebral osteomyelitis. AJR Am J Roentgenol 153(2):399–405
16. Hoffman EB, Crosier JH, Cremin BJ (1993) Imaging in children with spinal tuberculosis. A comparison of radiography, computed tomography and magnetic resonance imaging. J Bone Joint Surg Br 75(2):233–239
17. Liu GC, Chou MS, Tsai TC, Lin SY, Shen YS (1993) MR evaluation of tubercular spondylitis. Acta Radio 34(6):554–558
18. Kim NH, Lee HM, Suh JS (1994) Magnetic resonance imaging for the diagnosis of tuberculous spondylitis. Spine (Phila Pa 1976) 19(21):2451–2455
19. Shanley DJ (1995) Tuberculosis of the spine: imaging features. AJR Am J Roentgenol 164(3):659–664
20. al-Mulhim FA, Ibrahim EM, el-Hassan AY, Moharram HM (1995) Magnetic resonance imaging of tuberculous spondylitis. Spine (Phila Pa 1976) 20(21):2287–2292
21. Loke TK, Ma HT, Chan CS (1997) Magnetic resonance imaging of tuberculous spinal infection. Australas Radiol 41(1):7–12
22. Yusof MI, Hassan E, Rahmat N, Yunus R (2009) Spinal tuberculosis: the association between pedicle involvement and anterior column damage and kyphotic deformity. Spine (Phila Pa 1976) 34(7):713–717
23. Thrush A, Enzmann D (1990) MR imaging of infectious spondylitis. AJNR Am J Neuroradiol 11(6):1171–1180
24. Jung NY, Jee WH, Ha KY, Park CK, Byun JY (2004) Discrimination of tuberculous spondylitis from pyogenic spondylitis on MRI. AJR Am J Roentgenol 182(6):1405–1410
25. Jain AK, Aggarwal A, Mehrotra G (1999) Correlation of canal encroachment with neurological deficit in tuberculosis of the spine. Int Orthop 23:85–86
26. Joseffer SS, Cooper PR (2005) Modern imaging of spinal tuberculosis. J Neurosurg Spine 2(2):145–150
27. Mahboubi S, Morris MC (2001) Imaging of spinal infections in children. Radiol Clin North Am 39(2):215–222
28. Jain AK, Dhammi IK (2007) Tuberculosis of the spine: a review. Clin Orthop Relat Res 460:39–49
29. DeRoos A, van Persijn, van Meerten EL, Bloem JL, Bluemm AG (1986) MRI of tuberculous spondylitis. AJR Am J Roentgenol 146:79–82
30. Lindahl S, Nyman RS, Brismar J, Hugosson C, Lundstedt C (1996) Imaging of tuberculosis. IV. Spinal manifestations in 63 patients. Acta Radiol 37(4):506–511
31. Dhammi IK, Jain AK, Buxi TB (2002) Non-operative management of an intramedullary tuberculoma. Trop Doct 32:44–45
32. Jena A, Banerji AK, Tripathi RP et al (1991) Demonstration of intramedullary tuberculomas by magnetic resonance imaging: a report of two cases. Br J Radiol 64:555–557
33. Gillams AR, Chaddha B, Carter AP (1996) MR appearances of the temporal evolution and resolution of infectious spondylitis. AJR Am J Roentgenol 166(4):903–907
34. Jain AK, Jena AN, Dhammi IK, Kumar S (1999) Fate of intervertebral disc space in paradiscal tuberculous lesions. Indian J Orthop 33:90–94
35. Raja A (2004) Immunology of tuberculosis. Indian J Med Res 120:213–232